Problems in the physics of ion–atom collisions important for accelerator technology and alternative nuclear power

A. K. Kaminskiĭ
Institute of Nuclear Physics, Moscow State University, Moscow

A. A. Vasil'ev
Moscow Radiotechnical Institute, Russian Academy of Sciences, Moscow

Fiz. Élem. Chastits At. Yadra **29**, 489–518 (March–April 1998)

Some problems of accelerator technology and the practical use of high-intensity proton and ion beams for fundamental and applied research and nuclear power production based on the use of accelerated particle beams and subcritical reactors are briefly described. All these problems require detailed study of ion–atom collision physics. The main problems in developing theoretical methods for calculating the differential and total effective cross sections for processes occurring in fast ion–atom collisions, where the two colliding particles are multielectron systems, are discussed. Methods are given for the approximate calculation of the angular and energy distributions of ions and electrons in the ionization of multielectron ions and atoms with accuracy sufficient for practical applications. © *1998 American Institute of Physics.* [S1063-7796(98)00402-1]

1. INTRODUCTION

Already for several decades now, the leading nuclear reactor and accelerator centers around the world have been planning and carrying out projects which use high-intensity proton and ion beams to solve fundamental and applied problems in science and technology. The first high-intensity proton accelerators were meson factories,[1–4] in which beams of protons or negative ions H^- with an intensity of order 1 mA are accelerated to 600–800 MeV. The idea is that the accelerated ions H^- will be stripped for storage and change of the time structure of the beam.

Reducing the loss of beam intensity to a minimum has always been a serious problem in accelerator technology, but for high-intensity accelerators the problem becomes acute. In ordinary accelerators with relatively low intensity $I \leqslant 1\ \mu$A, an intensity loss of even ten percent in the acceleration and transport of the beam essentially just lengthens the time for performing an experiment and makes it necessary to increase the screening of areas sensitive to radiation. At high-intensity accelerators with $I > 1$ mA even much smaller intensity losses are incompatible with the strict requirements of radiation safety.

Calculations of the beam dynamics and the beam loss due to collisions with atoms of the residual gas require reliable values of the effective cross sections for the ionization, charge exchange, and scattering of the accelerated particles in collisions with atoms of the residual gas. This has made it necessary to perform detailed studies of the interaction processes occurring between the ions of the beam and the atoms of the residual gas and various charge-exchange targets at various energies of the accelerated protons and ions. It has also made it necessary to develop sufficiently accurate approximation methods for calculating the corresponding effective cross sections, since the experimental data and calculations of such cross sections at energies $E/A \geqslant 10$ MeV/nucleon are only fragmentary.[5–12] Improvement of the vacuum in the accelerator channel and the transport of high-energy ion beams has made the problem of accurately determining the effective cross sections for ion charge exchange and scattering on residual gas atoms less acute, because these cross sections fall off rapidly with increasing energy.

However, the effective cross sections for ionization and electron capture in ion–atom and electron–atom collisions remain important for the development of modern ion sources and injectors,[13–16] and also for calculations of various charge-exchange schemes and for the corresponding targets. In existing and planned plasma ion sources a powerful beam of laser or superhigh-frequency radiation effectively ionizes the atoms of practically any element, but the problem of extracting a sufficient intensity of highly charged ions from the plasma cloud is very complicated. During extraction from the plasma cloud highly charged ions (ions with a high degree of ionization) capture plasma electrons and effectively decrease their charge. No theoretical model has yet been constructed for this process.[16] Therefore, the use of charge-exchange targets for increasing the charge of the accelerated ions becomes essential in choosing an optimal design for a charged-ion accelerator.

Knowledge of the effective charge-exchange cross sections of negative ions is also required for ion accelerators of the widely used direct-action, tandem type, where a positive potential is supplied to a central electrode, while the injector and beam extraction apparatus are held at zero potential. The stripping of negative ions to states with positive charge occurs in a charge-exchange target located at the center of the accelerator.

The choice of charge-exchange target and the determination of its parameters are very important for designing the accelerator. The parameters of the gaseous target determine

the parameters of the vacuum system of the accelerator and the cost of running it. These considerations are also important for another type of accelerator, where the injection assembly contains several charge-exchange targets for the systematic stripping of ions after they have passed through the corresponding accelerator sections, producing further acceleration of the ions. These goals require the effective charge-exchange cross sections of a large number of ions on various targets and in a wide range of energies.

Study of the interactions of H^- ions with various atoms has allowed the determination of the vacuum required in the chambers of a future meson factory, the efficiency and lifetime of various charge-exchange targets, and the increased emittance of the beam in multiple passages through the charge-exchange target for multiturn injection into the storage ring.[17–23] In particular, it has been shown that the lifetime of the charge-exchange target of a meson factory is determined by the accumulation of radiation damage in the bombarded part. The possibility of using charge-exchange electron diagnostics of a high-intensity H^- ion beam has also been demonstrated.[21]

Several institutes are developing projects in which intense proton and ion beams will be used for inertial controlled thermonuclear fusion,[24–28] and there are proposals for the use of hydrostatic compression of deuterium and tritium targets acted on by powerful ion pulses. The design and construction of accelerators with the required parameters is extremely complicated and requires important preliminary studies of many aspects, including the interactions between the beam ions and the target.

Problems of the interaction of intense electron and γ beams with atomic targets which are in some respects similar to those described above also are important for carrying out projects on electron and laser variations of inertial thermonuclear fusion.

Ion beams are used to raise the plasma temperature in tokamaks, where the problem also arises of minimizing the temperature decrease of the plasma owing to collisions of electrons with ions knocked out of the front wall.

Another important application of intense proton and light-ion beams was and still is the problem of creating high-intensity neutron sources[29–42] for the electronuclear method of producing and using up nuclear fuel, for the transmutation of long-lived nuclear wastes from atomic power plants and other nuclear reactors, and so on. Several authors[32,34] have studied the possibility of using accelerated ion beams for this, as the neutron yield per accelerated particle is higher than for proton beams. A direct outcome of these studies was the projects carried out at several institutes for using intense neutron beams, created in collisions of intense proton or ion beams with the atoms of various targets, for the construction of subcritical nuclear reactors with preliminary neutron irradiation.

The use of intense proton and ion beams in nuclear power reactors operating in the subcritical regime allows the solution of a number of problems in nuclear safety. Some of the technical problems of designing atomic power plants based on subcritical reactors have been worked out, and the economic competitiveness of such power plants compared to ones based on traditional reactors has been estimated.[42–44] According to several authors, the creation of an atomic power plant producing a power of order 1 GW using reactors operating in the subcritical regime requires accelerators with proton energy of order 1 GeV and intensity of the order of tens or hundreds of milliamperes, depending on the reactor features and the degree of subcriticality. Therefore, the intensity of an accelerator used to control a subcritical reactor at an atomic power plant must be about two orders of magnitude higher than that of one operating at existing meson factories. This further tightens the requirements on minimizing the loss of beam intensity during acceleration and transport.

A fundamental technical problem in realizing such atomic power plants is the creation of economical and reliable high-current proton and ion accelerators. Working out the technical foundations for constructing accelerators with an energy of about 1 GeV and a current of tens or hundreds of milliamperes is a complicated problem. Given the efficiency of extracting such intense accelerated beams, it is preferable to focus on linear accelerators with warm or superconducting structures,[45,46] although some authors also consider the possibility of using ring accelerators.[44,47–49] The creation of such accelerators requires the solution of a number of problems associated with the interaction of the accelerated ions with the residual gas, the accelerator walls, and various targets.

Along with pursuing the possibilities of existing accelerator designs, it is important to continue studying new acceleration techniques which can provide a significantly higher rate of acceleration. The interaction of high-power laser radiation and an intense electron beam appears promising for the development of new accelerator designs. One possible approach is to use the oscillations arising in a plasma acted on by radiation from one or two lasers at close frequencies or a powerful electron beam. The development of new types of high-power laser with a power of tens of terawatts has led to studies on the second generation of plasma accelerators.[50] The design and construction of such accelerators require study of the propagation of laser radiation and an electron beam in a plasma.

The development of the technology for the reactors discussed above requires theoretical and experimental study of the various mechanisms by which proton and ion beams interact with the materials of the active zone, the effective nuclear reaction cross sections and the energy lost to ionization and excitation of the atoms for various targets, and the angular, energy, and charge distributions of all the particles after collisions. This information is required not only for selecting the energy and intensity of the accelerator beam, but also for determining the optimal structure of the target, taking into account the allowed thermal stresses and so on.

Reliable calculations of the energy loss in ion–atom collisions are required for many applied problems. At present there are accurate approximation methods for calculating the energy loss in elementary collisions of the simplest ions (hydrogen, helium) in rarefied gaseous targets of light atoms. It is necessary to be able to perform such calculations also for various ions in gaseous targets of various densities, and in

solid and monocrystalline targets of various thicknesses, taking into account the density effect. In dense media, ions excited in a collision do not manage to deexcite before the next collision, and the characteristics of such collisions are quite different.

Ions with weakly bound electrons (for example, H^- ions or other negatively charged ions) have sizes comparable to or even larger than the interatomic spacings in dense targets. In interactions with incident ions, the mechanism for the ionization of weakly bound outer electrons of metallic targets differs significantly from that for the ionization of tightly bound atomic electrons.

The energy losses of ions channeled in monocrystals differ qualitatively from the losses in amorphous media. Study of the dependence of the probability for a process on the impact parameter can prove useful in this case.[51,52]

The values of the ion energy loss in various targets are needed, in particular, to study radiation damage and the mechanisms leading to the breakdown of irradiated targets, for estimating the lifetime of such targets, and for developing a number of new industrial technologies.[53] Low-intensity proton and ion beams have long been used in medicine for producing nuclear isotopes and curing malignant tumors.[54–57]

Only fragmentary experimental data on the problems listed above can be found in the literature. Systematic studies must be performed in order to develop reliable theoretical methods for dealing with these problems.

At ion energies $E/A > 10$ MeV/nucleon, detailed studies of the ionization processes are of primary importance for practical applications in accelerator technology. The effective cross sections for electron capture at these energies are needed only in solving problems involving ion sources.

Investigations of the structure and composition of materials can be performed by the inverse scattering method and by studying the angular, energy, and charge distributions of ions after scattering at large angles on various amorphous and monocrystalline targets.[58,59]

Here we shall present methods for calculating the effective ionization cross sections in ion–atom collisions and the angular and energy distributions of ions and electrons after such collisions, and compare the results with the experimental data. The results of work on some of the other problems listed above and related problems will be published in a subsequent study.

2. FEATURES OF METHODS OF CALCULATING THE EFFECTIVE CROSS SECTIONS FOR CHARGE-EXCHANGE PROCESSES IN ION–ATOM COLLISIONS

As mentioned above, the solution of a number of applied problems requires knowledge of the total and differential effective cross sections for ionization and electron capture in collisions of ions of energy E, nuclear charge z_A, and ion charge i_A (for a wide range of values of these quantities) with the atoms of various targets. Only fragmentary data on these cross sections are available in the literature. There is no unified theory of such collisions for the entire range of parameters, and the construction of such a theory encounters both fundamental and computational difficulties.

The mathematical techniques useful in the theory of atomic collisions and a description of the relevant approximations can be found in Ref. 60. However, the treatment there is rather awkward and encumbered with mathematical formalism, and for practical applications it is necessary to analyze new experimental data and develop computational methods suited to the purposes described above in the Introduction. Such an analysis is also necessary because the vast majority of studies in the physics of ion–atom collisions have been performed at fairly low energies, in the region where the effective cross sections for these processes are maximal, i.e., at incident particle velocities close to those of the atomic electrons. For incident ions this corresponds to an energy of order 10 keV/nucleon. This is a consequence of the possibilities offered by existing accelerators, and also the fact that at low energies these cross sections are maximally informative about the collision mechanisms, the applicability of various approximations for describing the wave functions of multielectron systems, and, more generally, the construction of theoretical approximations for solving the many-body problem with long-range potentials in quantum mechanics.

At ion velocities low compared to the velocities of atomic electrons, the basic theoretical method is the quasimolecule method.[61] A full description of this method lies outside the scope of the present study. We only note that it gives correct results, and that it describes electron transitions using the laws of quantum mechanics, which requires quite lengthy and tedious calculations.

The physics of fast ion–atom collisions possesses special features which make it relatively easy to develop approximation methods for calculating the cross sections for effective ionization and other processes.

Let us point out some of the characteristic features of ion–atom collisions at high and intermediate energies which are important for choosing theoretical approximations and which are determined by the energy and momentum conservation laws and the purely Coulomb interaction of all the particles involved in the collision (atomic nuclei and all the electrons of the incident ion and target atom).

As a rule, in processes associated with the rearrangement of electron shells and electron loss or capture the fast incident ion loses only an insignificant part of its energy E and momentum $\mathbf{p}$ ($\Delta E \ll E$ and $\Delta \mathbf{p} \ll \mathbf{p}$). The transferred energy ΔE is usually comparable in order of magnitude with the ionization potential of the corresponding shell of the atom or ion, amounting to tens or hundreds of eV for outer shells. Large losses ΔE are therefore unlikely, as are large $\Delta \mathbf{p}$. Therefore, in such collisions ions are scattered at small angles $\theta \approx \Delta p/p$. Large scattering angles θ correspond to processes associated with the rearrangement of the inner shells of heavy atoms. Large-angle scattering of the ions occurs only in scattering on nuclei of the target in collisions with small impact parameters.

Meanwhile, owing to the slow falloff of the Coulomb potential with distance, in any collision there is a significant probability for the states of several electrons to change in a single collision.

Even in distant collisions, when the state of only a single weakly bound electron is changed, this transition occurs as a result of the interaction of all the Coulomb centers, i.e., the two nuclei and all the electrons. This means that the calculation of the effective cross sections of ion–atom processes always requires the solution of the quantum-mechanical many-body problem. At present it is possible to develop approximation methods for solving this problem only by using special models and approximations which are applicable in only a limited range of parameters (energy, charge, degree of ionization, and so on), and so it is very difficult to estimate the accuracy of such calculations. The existing approximation methods developed for potentials which fall off rapidly with distance and which allow the solution of a number of problems in nuclear physics are inapplicable here, owing to slow falloff of the potential.

An important feature of the effective cross sections of ion–atom collisions is the presence of a sizable energy range in which the energy dependence of the cross sections can be described by asymptotic expressions. At ion velocities v exceeding the orbital velocity of the ejected electron, the effective ionization cross sections asymptotically approach the dependence v^{-2}, while the energy dependence of the electron capture cross sections is considerably stronger.

The spin functions and identical nature of the electrons are taken into account in the correct treatment of the symmetry properties of the initial- and final-state wave functions of the ions and atoms. Polarization effects are not important in these problems, and nuclear forces do not participate in the interaction at distances of order $(10^{-8}-10^{-7})$ cm, which give the dominant contribution to the cross sections.

Owing to these features of fast ion–atom collisions, the physically correct methods of calculating the effective ionization cross sections are based on the use of various versions of perturbation theory. The solution of problems involving many particles with spin and coupled by a weakly decreasing interaction potential, as in our case here, requires the introduction of several approximations based on the physical understanding of the problem.

A system of an ion plus an atom is described by a wave function Ψ which is a solution of the Schrödinger equation

$$-i\hbar\frac{\partial\Psi}{\partial t}=H\Psi. \tag{2.1}$$

In perturbation theory the Hamiltonian H is split into two parts

$$H=H_0+U, \tag{2.2}$$

where H_0 describes the free ion and atom (their motion and structure), and the interaction operator

$$U=\frac{z_Az_Be^2}{|\mathbf{R}|}-\sum_{j=1}^{z_B}\frac{N_Ae^2}{|\mathbf{R}-\mathbf{r}_j|}-\sum_{l=1}^{N_A}\frac{z_Be^2}{|\mathbf{R}+\mathbf{r}_l|}+\sum_{j=1}^{z_B}\sum_{l=1}^{N_A}\frac{e^2}{|\mathbf{R}+\mathbf{r}_l-\mathbf{r}_j|} \tag{2.3}$$

describes the interaction of the two nuclei and all the electrons with an "external" nucleus. Here and below, $\mathbf{r}_j$ and $\mathbf{r}_l$ are the radius vectors of the target and ion electrons (relative to their nuclei), respectively, and $N_A=z_A-i_A$ is the number of electrons of the ion.

The main complexity of the problem is the lack of an exact solution of the equation

$$H_0\Psi=E\Psi \tag{2.4}$$

and the fundamental difficulties of finding one by approximation methods. An exact solution of the Schrödinger equation for the wave functions Ψ_A and Ψ_B of free ions and atoms exists only for the H atom and hydrogen-like ions. For atoms and ions with the number of electrons $N>1$ there exist only approximate wave functions Ψ_A and Ψ_B constructed in various bases, which can include tens or hundreds of basis functions. The need for such complicated functions arises in the detailed inclusion of electron correlations and configuration mixing in calculations of tiny effects in electron transitions (the optical-line widths, the structure of mesonic atoms, and so on). Of course, such calculations are very awkward.

For our purposes the initial and final states of the incident ion are important, while the electron states of the target atom can be summed over. In general, the effective cross section for the inelastic scattering of an incident ion is given by the expression from the general theory of inelastic scattering:[62]

$$d\sigma=\frac{M_iM_fp_f}{(2\pi\hbar^2)^2p_i}|\langle\Phi_f|T|\Phi_i\rangle|^2d\Omega. \tag{2.5}$$

Here M_i and M_f are the masses of the ion scattered into solid angle $d\Omega$ before and after the collision, respectively, $\mathbf{p}_i$ and $\mathbf{p}_f$ are the corresponding momenta, and Φ_i and Φ_f are the wave functions of the initial and final states of the system. In calculations of the effective ionization cross sections, $d\Omega$ in (2.5) must be replaced by $d\Omega d\varepsilon d\omega$, because in the final state along with undergoing scattering in solid angle $d\Omega$, an electron of energy ε is ejected into a solid angle $d\omega$ by the ion.

Equation (2.5) is exact. The fundamental information about the process is contained in the matrix elements of the T matrix, and it is in calculating them that the approximations mentioned above are made (structure formulas are used to expand the T matrix in a series, but convergence of the series is not guaranteed). For a system of an ion plus an atom even the construction of the initial and final wave functions Φ_i and Φ_f is possible only by using an approximation with limited accuracy.

All the intermediate calculations are most conveniently carried out in the center-of-mass frame, assuming $M_i=M_f$ and neglecting the electron mass m compared to the masses of the ion and the atom.

The main working approximation in calculations of the ionization cross sections in fast ion–atom collisions is the plane-wave Born approximation (PWBA), in which the wave functions Ψ_i and Ψ_f of the initial and final states of the system have the form

$$\Psi_i=\Psi_{Ai}\Psi_{Bi}\exp(i\mathbf{p}_i\mathbf{R}/\hbar),$$
$$\Psi_f=\Psi_{Af}\Psi_{Bf}\exp(i\mathbf{p}_f\mathbf{R}/\hbar), \tag{2.6}$$

where Ψ_A and Ψ_B are the wave functions of the free states of the ion and atom, respectively, and $\mathbf{R}$ is the separation between the nuclei of the ion and the atom.

For practical calculations of the effective ionization cross sections in fast ion–atom collisions it is desirable to construct functions Ψ_A and Ψ_B which allow approximate values of the ionization cross sections to be obtained relatively simply and with accuracy sufficient for practical applications (of course, these functions will not be useful for calculating the tiny effects mentioned above). For this, the optimal functions are Ψ_A and Ψ_B in the form of linear combinations[63]

$$\Psi_A(\mathbf{r}_1,\mathbf{r}_2,\ldots\mathbf{r}_{N_A})=\sum_t \alpha_t \prod_{j=1}^{N_A} \Psi_j(z_j,\mathbf{r}_j)\chi_j(m_{sj}) \qquad (2.7)$$

of one-electron Coulomb wave functions

$$\Psi_j(z_j^*,\mathbf{r}_j)=R_{nl}(z_j^*,r_j)Y_{lm}(\theta_j,\varphi_j) \qquad (2.8)$$

and spin functions $\chi_j(m_{sj})$.

The coefficients α_t are chosen such that Ψ_A and Ψ_B correspond to the ground-state quantum numbers of the ion and atom, respectively: the total angular momentum J, the orbital angular momentum L, and the spin S, and the required symmetry properties and satisfaction of the Pauli principle are ensured.[64] The coefficients α_t consist of combinations of the corresponding coefficients of the vector addition of the angular momenta; for brevity, we shall not write them out here.

The functions (2.8) are mutually orthogonal, owing to the orthogonality of the spherical harmonics $Y_{lm}(\theta_j,\varphi_j)$. The exception is the ns states, which require additional orthogonalization. The radial functions $R_{nl}(z_{nl}^*,r)$ for different shells are not orthogonal, as they differ by the values of the effective charges z_{nl}^*.

In this approximation the operator (2.3) is a single-particle operator with respect to the electrons of the ionized ion A, and so in a first approximation only the state of a single electron can change (this includes ejection into the continuum). The effective cross section for multiple ionization is zero in this approximation. It can be described only by more complicated higher-order expressions.

3. CALCULATION OF EFFECTIVE IONIZATION CROSS SECTIONS IN ION–ATOM COLLISIONS

3.1. Calculation of the ion angular distributions after ionization in ion–atom collisions

The effective ionization cross section $d\sigma_A/d\Omega$ of an incident ion A in a collision with an atom B, differential in the scattering angle θ (i.e., after ejection of an electron from the initial state $|nlm\rangle|\frac{1}{2}m_s\rangle$ of the ion into the continuum), has the following form in the approximation that we have described:[63]

$$\frac{d\sigma_A}{d\Omega}=\frac{d\sigma_A^{el}}{d\Omega}+\frac{d\sigma_A^{in}}{d\Omega}, \qquad (3.1)$$

$$\frac{d\sigma_A^{el}}{d\Omega}=\frac{4a_0^2z_B^2M^2}{z_A^{*4}m^2}\int\left[1-\frac{N_B}{z_B}F_B(q)\right]^2\frac{v'\eta_{nlm}(q,k)dk}{vq^4}, \qquad (3.2)$$

$$\frac{d\sigma_A^{in}}{d\Omega}=\frac{4a_0^2N_BM^2}{z_A^{*4}m^2}\int S_B(q)\frac{v'\eta_{nlm}(q,k)dk}{vq^4}. \qquad (3.3)$$

Summation of Eqs. (3.1)–(3.3) over the initial states of the N_A electrons gives the angular distribution of the ions A after ionization (loss of any of the N_A electrons of the ion A), and integration of this sum over the momentum k and angle Ω gives the total cross section σ for ionization of the ion in a collision with the atom B. Here and below, we use the notation $d\Omega=2\pi\sin\theta\,d\theta$, M is the reduced mass of the colliding ion A and the atom B, v and v' are their relative velocities before and after the collision, q is the change of momentum of the incident ion, k is the electron momentum in the coordinate frame attached to the ion A, $\eta_{nlm}(q,k)$ is the squared modulus of the matrix element $\varepsilon_{nlm}(q,\mathbf{k})$ for the electron transition from the state $|nlm\rangle$ to the continuum, integrated over the emission angle χ of the ejected electron, m is the electron mass, $a_0=5.29\times10^{-9}$ cm is the Bohr radius, z_A^* is the effective charge of the ionized shell of the ion A, and the quantities q and k are given in units of $z_A^*\hbar a_0^{-1}$.

The relation between the scattering angle θ and the quantities q and k is determined by the conservation laws. We shall discuss this in more detail below.

The form factors $F_B(q)$ and $S_B(q)$ are determined[65] by only the electronic structure of the atom (or ion) B, described by its initial function $\Psi_{Bi}(\mathbf{r}_1,\mathbf{r}_2,\ldots,\mathbf{r}_{N_B})$:

$$F_B(q)=N_B^{-1}\sum_{j=1}^{N_B}\int|\Psi_B|^2\exp(i\mathbf{q}\mathbf{r}_j/\hbar)d\mathbf{r}, \qquad (3.4)$$

$$S_B(q)-N_B^{-1}\left[\sum_{i\neq s}^{N_B}\int|\Psi_B|^2\exp(i\mathbf{q}(\mathbf{r}_j-\mathbf{r}_s)/\hbar)d\mathbf{r}-|N_BF_B(q)|^2\right]. \qquad (3.5)$$

The integration in (3.4)–(3.5) runs over all the radius vectors $\mathbf{r}_j$ of all N_B electrons of the atom B.

For many atoms and some ions there are tables in the literature[66–69] which give the form factors $F_B(q)$ and $S_B(q)$ calculated using various wave functions. However, it is more convenient to use analytic expressions for $F_B(q)$ and $S_B(q)$. These are given and discussed in Ref. 59 for atoms with $z_B\leqslant7$ and ions with $N_B\leqslant7$. The expressions for $F_B(q)$ and $S_B(q)$ calculated using the wave functions (2.7) and (2.8) for atoms with $z_B\leqslant10$ and ions with $N_B\leqslant10$ have the form[70]

$$F(q)=N^{-1}[N_{1s}L(1s,1s)+N_{2s}L(2s,2s)+N_{2p_0}L(2p_0,2p_0)+N_{2p_1}L(2p_1,2p_1)], \qquad (3.6)$$

$$S(q)=N^{-1}[N-a_1L^2(1s,1s)-a_2L^2(2s,2s)-a_3L^2(1s,2s)-a_4L^2(2p_0,2p_0)-a_5L^2(2p_1,2p_1)-a_6L^2(1s,2p_0)-a_7L^2(2s,2p_0)-a_8L(2p_0,2p_0)L(2p_1,2p_1)]. \qquad (3.7)$$

The values of the one-particle matrix elements

TABLE I. Values of the coefficients a_i in Eq. (3.7) for the inelastic form factor $S(q)$ for an ion or atom with $N \leqslant 10$.

N	Term	a_1	a_2	a_3	a_4	a_5	a_6	a_7	a_8
1	$^2S_{1/2}$	1							
2	$^1S_0$	2							
3	$^2S_{1/2}$	2	1	2					
4	$^1S_0$	2	2	4					
5	$^2P_{1/2}$	2	2	4	1/9	4/9	2/3	2/3	4/9
6	$^3P_0$	2	2	4	4/9	10/9	4/3	4/3	4/9
7	$^4S_{3/2}$	2	2	4	1	2	2	2	
8	$^3P_2$	2	2	4	10/9	22/9	8/3	8/3	4/9
9	$^3P_{3/2}$	2	2	4	13/9	28/9	10/3	10/3	4/9
10	$^1S_0$	2	2	4	2	4	4	4	

$$L(nlm,n'l'm') = \int \Psi^*_{nlm}(\mathbf{r}) e^{i\mathbf{qr}/\hbar} \Psi_{n'l'm'}(\mathbf{r}) d\mathbf{r} \quad (3.8)$$

are given in Ref. 70 and in the Appendix.

The coefficients N_{1s} and N_{2s} are the numbers of electrons in the $1s$ and $2s$ shells of the ions or atoms, respectively. The coefficients N_{2p_0} and N_{2p_1} are

$$N_{2p_0} = (N-4)/3, \quad N_{2p_1} = 2(N-4)/3. \quad (3.9)$$

In obtaining (3.9) we have used the fact that the matrix elements (3.8) with $m=+1$ and $m=-1$ are equal, and only transitions with different values of m are forbidden.

The coefficients a_i in (3.7) are given for various ions in Table I, where the blank spots correspond to coefficients equal to zero.

In Fig. 1 we show the form factors $F_B(q)$ and $S_B(q)$ of the oxygen atom O and the O^{+2}, O^{+3}, and O^{+6} ions, calculated in various approximations. The form factors for light atoms tabulated in Ref. 69 agree better with those calculated using the analytic expressions from Ref. 70 with the variational values of z^*_{nl} from Ref. 71 than with those obtained from the binding energy in Refs. 72 and 73.

In analyzing the effect of the elastic form factor $F_B(q)$ on the cross sections it is more convenient to consider, rather than $F_B(q)$, the quantity appearing in (3.2):

$$U_i(q) = [1-(N_i/z_i)F_i(q)]^2. \quad (3.10)$$

Let us discuss some of the properties of $U_i(q)$ and $S_i(q)$ for atoms and ions.

For any ionizing atom or ion, $U_i(q) \to 1$ at large q, owing to the small screening of the ionizing nucleus by its electrons at large scattering angles.

In distant collisions with small q the screening of the nucleus B depends on the degree of ionization $(z_B - N_B)$. In atom–atom collisions the screening of the nuclei at small q is complete, and for $q \to 0$ we have $U_i(q) \approx \alpha q^4$. If the ionizing ion is an ion of charge $(z_i - N_i)$, then at small q the quantity $U_i(q)$ tends not to zero, as for an atom, but to $(z_i - N_i)^2/z_i^2$. Therefore, in distant collisions $d\sigma/d\Omega$ corresponds to ionization by a nucleus of charge $(z_i - N_i)$.

The shell structure of the ionizing atom or ion is manifested in the curves $U_i(q)$ and $S_i(q)$ as characteristic bends at intermediate values of q. The quantity $S_i(q)$ is more sensitive to the choice of wave functions than is $U_i(q)$ or $F_i(q)$.

The momentum transfer q is given by

$$q^2 = \frac{a_0^2 M^2}{z_i^{*2}\hbar^2}(v^2 + v'^2 - 2vv' \cos\theta). \quad (3.11)$$

Here v' is defined by the law for energy conservation:

$$v^2 - v'^2 = 2\Delta E M^{-1}. \quad (3.12)$$

The change of the energy ΔE in the collision is given by

$$\Delta E = I_A + k^2 z_A^{*2}\hbar^2/2ma_0^2 \quad (3.13)$$

in calculations of the quasielastic part of the cross section (3.2), and is equal to

$$\Delta E = I_A + \bar{I}_B + k^2 z_A^{*2}\hbar^2/2ma_0^2 \quad (3.14)$$

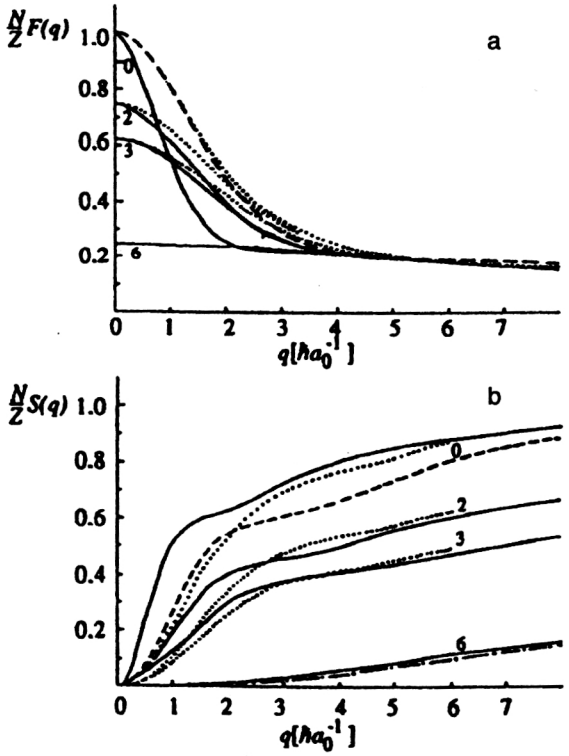

FIG. 1. Values of $NZ^{-1}F(q)$ (a) and $NZ^{-1}S(q)$ (b) for the oxygen atom and its ions. The solid curves show calculations with z^*_{nl} from the subshell binding energies,[72,73] and the dashed curve is calculated with variational z^*_{nl} (Ref. 71). The dotted curves show the data of Ref. 69, and the dot–dash curve shows the data of Ref. 71a. The ion charges are indicated near the curves.

for the quasi-inelastic part (3.3). Here I_A denotes the binding energy of the electron ejected from the ion A, and $\bar{I}_B$ denotes the average excitation energy of the atom B.

In contrast to the binding energies I_A and I_B of an electron in the ion and atom, respectively, $\bar{I}_B$ is not a strictly defined quantity. The ionization differential cross section $d\sigma/d\varepsilon d\Omega$ and total cross section σ calculated from the above expressions depend weakly on the choice of $\bar{I}_B$, and the average ionization potentials from Ref. 74 can be used in the calculations. Meanwhile, in calculating the electron spectra $d^2\sigma/d\varepsilon d\omega$, which are studied below, use of the sum rule[65] gives satisfactory agreement with the calculations using direct summation over states of the ionizing atom with $\bar{I}_B$ chosen as[75]

$$\bar{I}_B = I_B + k^2 z_A^{*2}\hbar^2/2ma_0^2 . \tag{3.15}$$

Equations (3.11)–(3.14) are given in the nonrelativistic approximation. Expressions for the ionization differential cross sections at moderately relativistic energies of the colliding ions, $E/A \leqslant 1$ GeV/nucleon, are given in Ref. 22.

Analytic expressions for $\eta_{nlm}(q,k)$ for K, L, and M electrons can be found in Refs. 76–78. These quantities completely determine the effective ionization cross section of a charged particle [for $F_B(q)=S_B(q)=0$], and are related as

$$\frac{dF(q,\Delta F)}{d(\Delta E)} = \frac{\Delta E}{I_0}(qa_0)^{-2}\eta_{nlm}(q,k) \tag{3.16}$$

to the density of the generalized oscillator strengths $dF(q,\Delta E)/d(\Delta E)$. The latter has been studied in sufficient detail both theoretically and experimentally[79] for K-electron ejection. The density of the generalized oscillator strengths is usually depicted as the Bethe surface $F(x,y)$ in three-dimensional space (with $\Delta E/I_0$ plotted on the x axis and $\ln[(qa_0)^2]$ on the y axis).

Let us mention two qualitative features of the Bethe surface which are illustrated in detail in Ref. 79.

The surface has a clearly expressed maximum at small x and y and decreases rapidly with increasing x and y. This maximum corresponds to scattering at small angles θ and can be studied experimentally in photoionization. The shape of the theoretically calculated maximum depends on the accuracy of the wave functions used to describe the initial and final states of the ejected electron.

A second feature of the Bethe surface is the presence of a ridge at values of k which are not too small [for $(qa_0)^2 = \Delta E/I_0$)]. This corresponds to near collisions of the ionizing particle with the ejected electron, referred to as binary collisions. The accuracy of describing such collisions depends relatively weakly on the wave functions used.

The characteristic features of the ion angular distributions $d\sigma/d\Omega$ after ionization in ion–atom collisions are seen from the results, presented in Fig. 2 from Ref. 63, of calculating $d\sigma/d\Omega$ for hydrogen atoms and protons of energy $E = 2$ MeV after collisions with C and H atoms. For comparison, we give the cross sections $d\sigma_y/d\Omega$ for the elastic scattering of hydrogen atoms and protons on ions and carbon atoms and the cross section $d\sigma_M/d\Omega$ for scattering on a

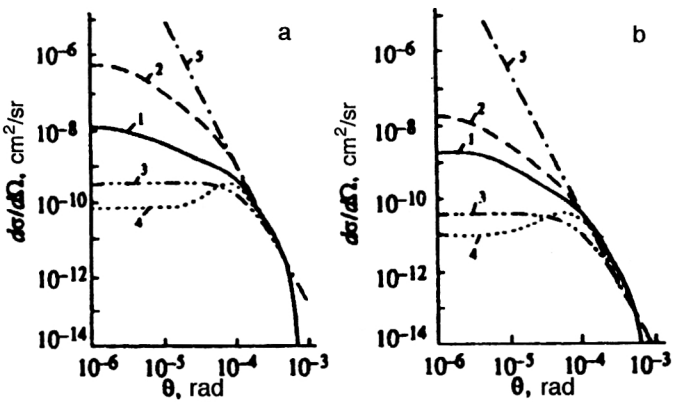

FIG. 2. Angular distributions $d\sigma_A/d\Omega$ of hydrogen atoms and protons with energy $E=2$ MeV after collisions with target atoms of carbon (a) and hydrogen (b). Curves *1* and *2* show $d\sigma_A/d\Omega$ for ionization of a hydrogen atom in a collision with a target atom and nucleus, respectively, curve *3* shows $d\sigma_{Ry}/d\Omega$, curve *4* shows $d\sigma_M/d\Omega$, and curve *5* shows $d\sigma_R/d\Omega$.

model potential. The cross section $d\sigma_y/d\Omega$ describes the elastic scattering of the incident atom with summation over the final states of the scattering atom:

$$\frac{d\sigma_y}{d\Omega} = \frac{d\sigma_R}{d\Omega}[U_A(q)U_B(q) + (q/q')^4 U_A(q)(N_B \times z_B^{-1})S_B(q')]. \tag{3.17}$$

Here $d\sigma_R/d\Omega$ is the Rutherford cross section for the scattering of the nucleus of A on the nucleus of B, $U_A(q)$ and $U_B(q)$ are given by (3.10) for the incident ion or atom A and the ionizing atom (or ion) B, and q and q' are given by Eqs. (3.11)–(3.15) for $I_A=0$ and $k=0$.

Three characteristic ranges of the angle θ can be distinguished[63] for the effective ionization cross sections $d\sigma/d\Omega$. At small θ the ionization cross section $d\sigma/d\Omega$ exceeds the cross section $d\sigma_y/d\Omega$ for the elastic scattering of the ion A on the atom B, and the larger $d\sigma/d\Omega$, the larger the degree of ionization of the target.

For $\theta > \theta_1$, where $\theta_1 = mv_0 z^*(Mv)^{-1}$, the values of $d\sigma/d\Omega$ are close to the Rutherford values. Beginning at some value θ_2, the calculated $d\sigma/d\Omega$ fall off more strongly with increasing θ than do the Rutherford cross sections $d\sigma_R/d\Omega$. However, the method described above becomes inapplicable at such large angles, because in such near collisions the relative motion of the nuclei of A and B cannot be described by the plane waves in (2.6). There are methods of taking this effect into account (distortions of plane waves or deviation of the incident ion trajectory from a straight line in terms of the classical description). However, for the class of problems considered here this effect is not important, because at such large scattering angles the cross section $d\sigma/d\Omega$ is many orders of magnitude smaller than at small θ.

Comparison of the cross sections $d\sigma/d\Omega$ for the ionization of hydrogen atoms with energy 2 MeV on H and C atoms[63] with the analogous calculations[80] at $E=300$ keV shows that the range $\theta_1 < \theta < \theta_2$ grows with increasing collision velocity.

For $v \leqslant z_{nl}^* v_0$, θ_2 tends to θ_1 and the Rutherford segment in $d\sigma/d\Omega$ disappears. At large collision velocities

$v > z_{nl}^* v_0$ the angular distributions of elastically scattered ions are considerably broader than the distributions $d\sigma/d\Omega$ for ionization of the outer shell.

Integration of Eqs. (3.1)–(3.3) over the angle Ω and summation over shells $|nlm\rangle$ gives the total cross section σ in ion–atom collisions. The satisfactory agreement between the values of σ calculated in the first Born approximation for collisions of protons and nuclei with target atoms and the experimental data at energies $E/A > 1$ MeV/nucleon was known earlier,[79] and it served as an additional stimulus for developing the method described above for calculating the ionization differential cross sections in fast ion–atom collisions.

3.2. Calculations of the spectra of electrons ejected in ion–atom collisions

The approximation described above has been used in a number of studies cited in Ref. 63 to calculate the cross sections doubly differential in the energy ε and emission angle $d\omega = \sin\chi d\chi d\varphi$ of an electron in ion–atom collisions.

Calculations of $d^2\sigma/d\varepsilon d\omega$, $d\sigma/d\varepsilon$, and $d\sigma/d\omega$ in ion–atom collisions must include the indistinguishability of the electrons ejected from the two ions or atoms A and B, each of which possesses its own electrons. In general, the fact that the electrons are identical significantly complicates the calculation of the electron spectra.

However, in fast ion–atom collisions it is possible to construct an approximation for calculating the electron spectra by using the available information about the structure of the doubly differential cross sections for the ionization of atoms by charged particles (electrons, protons, nuclei). We have noted above that the structure of $d^2\sigma/d\varepsilon d\omega$ in the ionization of atoms by fast charged particles is mainly determined by the structure of the squared modulus of the matrix element $\varepsilon_{nlm}(q,\mathbf{k})$ or the density of the generalized oscillator strengths (3.16). This structure is characterized by the presence of a clearly expressed maximum as $\varepsilon \to 0$ and a less intense ridge at velocities of the ejected electrons v_e close to $v_e = 2v\cos\chi$, where v is the velocity of the ionizing particle.

The target atom is usually at rest, and the coordinate system attached to the nucleus of the ionizing atom coincides with the lab frame, i.e., $\varepsilon = \varepsilon_L$. In ion–atom collisions this statement is valid for electrons ejected from the target atom, while electrons ejected from the incident ion experience a significant velocity transfer. Therefore, a significant fraction of the electrons ejected from the target atom will have laboratory velocity differing considerably from that of electrons ejected from the incident ion. We shall analyze this velocity distinction of the electrons in more detail below when we discuss the specific results.

This velocity distintinction of the electrons has led to the following model for calculating the electron spectra in fast ion–atom collisions.[22,63,81,82]

The doubly differential cross section for the ionization of a target atom B by an incident ion A is calculated from

$$\frac{d^2\sigma_B}{d\varepsilon d\omega} = \frac{d^2\sigma_B^{el}}{d\varepsilon d\omega} + \frac{d^2\sigma_B^{in}}{d\varepsilon d\omega}, \tag{3.18}$$

$$\frac{d^2\sigma_B^{el}}{d\varepsilon d\omega} = \frac{2a_0^2 z_A^2 v_0^2}{I_0 z_B^{*4} v^2} \int_{q_{\min}}^{q_{\max}} \left[1 - \frac{N_A}{z_A} F_A(q)\right]^2 kq^{-3}dq \int_0^{2\pi} \varepsilon_{nlm}^2(q,\mathbf{k})d\varphi, \tag{3.19}$$

$$\frac{d^2\sigma_B^{in}}{d\varepsilon d\omega} = \frac{2a_0^2 N_A v_0^2}{I_0 z_B^{*4} v^2} \int_{q_{\min}}^{q_{\max}} S_A(q) kq^{-3}dq \int_0^{2\pi} \varepsilon_{nlm}^2(q,\mathbf{k})d\varphi. \tag{3.20}$$

Here $I_0 = 13.6$ eV, $v_0 = 2.19\times 10^8$ cm/sec, and φ denotes the azimuthal scattering angle of the incident ion relative to the $(\mathbf{k}\cdot\mathbf{v})$ plane.

An important difference between Eqs. (3.18)–(3.20) and Eqs. (3.1)–(3.3) is the fact that in (3.2) and (3.3) it is possible to use the expressions $\eta_{nlm}(q,k)$ integrated over electron emission angles, while in (3.19) and (3.20) it is necessary to use the matrix elements $\varepsilon_{nlm}(q,\mathbf{k})$, which are not integrated over electron emission angles. In Eqs. (3.19) and (3.20) the relations (3.11)–(3.13) are real; only Eq. (3.13) for ΔE is replaced by (3.14), as noted above.

The matrix element $\varepsilon_{nlm}(q,\mathbf{k})$ calculated using Coulomb wave functions depends on the variables q, k, and the angle γ between the vectors $\mathbf{q}$ and $\mathbf{k}$, given by

$$\cos\gamma = \cos\theta_q \cos\chi + \sin\theta_q \sin\chi \cos\varphi, \tag{3.21}$$

where θ_q is the angle between the vectors $\mathbf{v}$ and $\mathbf{q}$, and

$$\cos\theta_q = \frac{z_B^* v_0 [M\Delta E (I_0 z_B^{*2})^{-1} + q^2 m]}{2mvq}. \tag{3.22}$$

The above procedure was used to calculate the doubly differential cross section $d^2\sigma_A/d\varepsilon d\omega$ in the coordinate frame attached to the incident ion A. For this only the locations of the indices A and B in Eqs. (3.19) and (3.20) are changed, and the corresponding constants, form factors, and matrix elements are substituted in the calculations. The resulting expression for $d^2\sigma_A/d\varepsilon d\omega$ is transformed into $d^2\sigma_A/d\varepsilon_L d\omega_L$ in a moving reference frame by using the equation[83]

$$\frac{d^2\sigma_A}{d\varepsilon_L d\omega_L} = \frac{v_L}{v_e}\frac{d^2\sigma_A}{d\varepsilon d\omega}. \tag{3.23}$$

If Eqs. (3.19) and (3.20) indicate a significant separation of the electrons from A and B in the energies ε_L, the total electron spectrum can be taken to be

$$\frac{d^2\sigma}{d\varepsilon_L d\omega_L} = \frac{d^2\sigma_A}{d\varepsilon_L d\omega_L} + \frac{d^2\sigma_B}{d\varepsilon_L d\omega_L}. \tag{3.24}$$

This method has been used to calculate $d^2\sigma/d\varepsilon d\omega$ for collisions of a number of light atoms and ions at various energies,[22,63,75,80–82] and to study the dependence of the cross sections on the initial state $|nlm\rangle$ of the ejected electron, on the energy and structure of the ionizing ion, and also the correctness of the sum rule. Comparison of the values of $d^2\sigma/d\varepsilon d\omega$ calculated in Ref. 81 for the ionization of nitrogen atoms by protons of energy $E = 1.7$ MeV with the experimental data from Ref. 84 has shown that these approximations are valid for the quantitative description of the

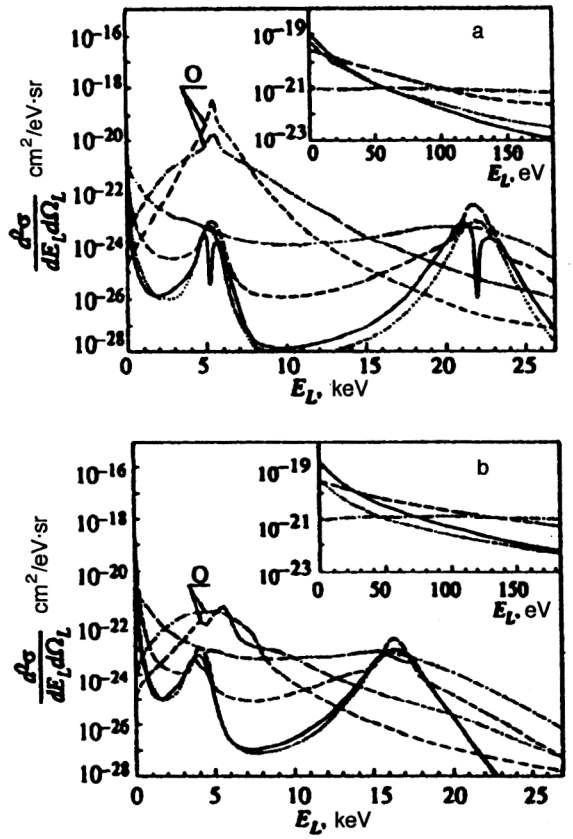

FIG. 3. Cross sections $d^2\sigma_A/d\varepsilon_L d\omega_L$ and $d^2\sigma_B/d\varepsilon_L d\omega_L$ as functions of the energy for collisions of the ion O^{+4} with energy $E/M=10$ MeV/nucleon with a target carbon atom. The electron is emitted at 1° (a) and 30° (b). The solid curves show the cross section $d^2\sigma_B/d\varepsilon_L d\omega_L$ for ejection of an electron from the initial state $2p_0$ of the carbon atom, the dotted curve is from the state $2p_1$, the dashed curve is from the state $2s$, and the dot–dash curve is from the state $1s$. The letter O marks the corresponding curves for the cross sections $d^2\sigma_A/d\varepsilon_L d\omega_L$ for knockout of electrons from the ion O^{+4}.

doubly differential cross sections for the ionization of atoms by charged particles even at such low energies. The validity of the approximation of summing the electron spectra from the incident ion A and the target atom B using Eqs. (3.22) and (3.23) has been demonstrated by the agreement (to within a factor of 2) of the values of $d^2\sigma/d\varepsilon_L d\omega_L$ calculated[22] and measured[85] in a wide range of energies ε_L and angles χ_L.

Let us discuss some of the characteristic features of the spectra of electrons ejected in fast ion–atom collisions, illustrated in Fig. 3 from Ref. 86 by the curves of $d^2\sigma/d\varepsilon_L d\omega_L$ for collisions of O^{+4} ions with $E/A=10$ MeV/nucleon with C atoms.

The electron spectra in all ion–atom collisions have narrow maxima at low energies $\varepsilon_L \to 0$ of the ejected electrons. These maxima are formed from the electrons ejected from the stationary target atoms in distant collisions with small energy transfer. Analogous maxima are observed in the ionization of atoms by nuclei.

The electron distribution at these maxima is practically isotropic in the electron emission angle χ_L, and the height of the maximum grows with increasing ion charge $(z_A - N_A)$.

The second characteristic feature of the electron spectra is the presence of a second sharp maximum at velocity v_L of the ejected electrons equal to the velocity v of the incident ion. This maximum is formed from electrons ejected from the incident ion and is characterized by a clearly expressed anisotropy, with the number of electrons falling rapidly with increasing angle χ_L. There is no such maximum in the spectra of electrons ejected in the ionization of atoms by nuclei.

The sharp distinction between these two maxima allows the electrons ejected from the different partners in the collision to be completely distinguished, and indicates that Eq. (3.24) is acccurate for such electrons. Moreover, the separation of these two maxima becomes even better as the velocity v of the incident ion increases.

Another feature of the electron spectra is the presence of two characteristic ridges. The first is located at $v_L = 2v\cos\chi_L$ and corresponds to electrons ejected from outer shells of the target atom in near (binary) collisions with the nucleus of the incident ion. The second ridge is located at $v_L = v\cos\chi_L$ and is formed by electrons ejected from the outer shells of the target atom in near collisions with the electrons of the incident ion.

As the incident ion energy E increases the inverted peaks between the different maxima increase and the separation of these groups of electrons improves. As the binding energy of the removed electron increases (in going to inner shells) the distinguishability of these maxima worsens and the structure of the spectra becomes less expressed. The ejection of electrons from the $|210\rangle$ (or $2p_0$) state gives rise to characteristic inverted peaks at the binary maxima (ridges) at $v_L = 2v\cos\chi_L$, owing to the negative parity of the state. The depth of these inverted peaks decreases with increasing angle χ_L.

It therefore follows that only for $v_L \approx v$ and $\chi_L \to 0$ do the electrons from the binary maximum at $v_L = v\cos\chi_L$ from the target atom B lie in the same region of ε_L and χ_L as the electrons ejected from the incident ion A. However, this is an extremely small fraction of the electrons ejected from the atom B, and so Eq. (3.23) is applicable for the vast majority of electrons.

The successful studies of the ionization differential cross sections has stimulated studies[87–89] of the triply differential effective cross sections $d^3\sigma/d\varepsilon d\omega d\Omega$.

3.3. The effective cross sections for multiple ionization in ion–atom collisions

The systematic study of multiple ionization processes in a single collision has just begun.[90–98] The above method of calculating the cross sections for single ionization is not directly applicable to multiple ionization, because the interaction operator (2.3) is a single-particle operator with respect to the ejected electron. Moreover, the use of the second Born approximation leads to very complex computational problems. Therefore, two schemes have been suggested for the semiquantitative calculation of the cross sections for double ionization in a single collision.

The first method is to transform[51] Eqs. (3.2)–(3.3) for the differential cross section $d\sigma/d\Omega$ for single ionization into a semiclassical ionization probability $W(x)$ depending

on the impact parameter x, after which the probability for double ionization $W(x)$ is taken to be the product

$$W^{(2)}(x)=W_1(x)W_2(x). \tag{3.25}$$

In this approximation the effective cross section for double ionization σ_2 is calculated by integrating (3.25) over x:

$$\sigma_2=2\pi\int W^{(2)}(x)xdx \tag{3.26}$$

and summing over sets of electron pairs. Comparison[90] of the cross sections σ_2 for double ionization of He atoms by protons calculated in this manner has shown that there is qualitative agreement with the experimental data[95] at proton energies $E\geqslant 10$ keV. Both the calculations and the experimental data indicate that σ_2 falls off more rapidly with increasing energy E of the ionizing particle than the E^{-1} behavior characteristic of σ for single ionization.

The second method of calculating the cross sections for double ionization assumes ejection into the continuum of an electron from an inner shell (while preserving the electrons in the outer shells) followed by transfer of excitation energy to one (or even two) electrons in the outer shells, which leads to ejection of an outer electron into the continuum. Here the probability for double ionization will be equal to the probability for single ionization of an inner shell of the atom times the probability for a transition from the resulting excited state followed by emission of a second electron. In this case the dependence of the cross section σ_2 on the energy E of the ionizing particle will be weaker and close to E^{-1}. It is also obvious that the maximum of the cross section σ_2 in this process will be shifted to higher energies E, as is characteristic of the ejection of electrons from deep inner shells with large binding energy.

It follows from the analysis of the cross sections for single ionization that the role of the second mechanism will decrease with increasing degree of ionization $(z-N)$ of the ionized particle. Physically, both processes are possible. They have not yet been studied in detail, either theoretically or experimentally.

The cross sections for multiple ionization do not play an important role in the acceleration and transport of beams in ion accelerators, because at energies $E/A>10$ MeV/nucleon these cross sections are much smaller than those for single ionization ($\sigma_2\ll\sigma$).

4. CONCLUSION

In Sec. 1 we explained why it is necessary to carry out detailed studies of the physics of ion–atom collisions in order to obtain the charge, angular, and energy distributions of all the particles, the ion energy loss as a function of the scattering angle in various targets, and so on, for various colliding ions and atoms in a wide range of energies. Experimental data on all these quantities is either completely lacking, or only fragmentary for particular colliding pairs at the edge of the energy range. The development of theoretical approximation methods for calculating these quantities encounters fundamental difficulties, as described in Sec. 2.

We have described a method of calculating the effective ionization differential cross sections in fast ion–atom collisions based on the first Born approximation, the sum rule, and a realistic choice of ion and atom wave functions [Eqs. (2.7)–(2.8)]. The assumption that the electrons ejected from different colliding particles can be distingished according to their energy[22,63,81,82] has turned out to be fruitful, as it makes it much easier to take into account the fact that the electrons are identical particles. In Sec. 3 we have presented a closed set of expressions and shown what results can be obtained from them.

Let us make a few comments about the accuracy of the method.

We have noted that it is difficult to obtain a rigorous quantitative estimate of the accuracy of the calculations for the entire parameter region using the general criteria of perturbation theory. Therefore, an important criterion for evaluating the accuracy in various parameter regions is comparison with the available experimental data. Such a comparison is particularly informative for the differential cross sections, as the results for a large family of curves are compared, rather than the single point for the total cross section. The comparison of the theoretical calculations of the doubly differential cross sections with the experimental data in Sec. 3 showed that this method gives results which agree with experiment to within a few tens of percent in a wide energy range of the ejected electrons, even for very moderate incident ion velocities. This agreement is observed right beyond the maximum of the total cross section, which came as a welcome surprise.

The effect of the electrons of the ionizing ion on the cross section for electron ejection from the ionizing atom (or ion) is automatically taken into account. This effect has been widely discussed in the literature,[99] and in qualitative analyses the term "screening effect" is used to refer to the decrease of the cross section for ionization by an ion compared to the cross section for ionization by a nucleus. The role of ionization of a target atom by electrons of the ionizing ion is referred to as "antiscreening." However, the correct quantitative inclusion of these effects is possible only when using the method described above.

We have given analytic expressions for the form factors $F(q)$ and $S(q)$ for ions and atoms with number of electrons $N\leqslant 10$, but the use of the wave functions in Eqs. (2.7) and (2.8) also allows such expressions to be obtained for large N.

Expressions for the matrix elements of the ionization of various shells using hydrogen-like wave functions are given in Ref. 61. They are very complicated.

The use of the first Born approximation does not introduce any inaccuracies into the effective cross sections at large incident ion energies. The inclusion of plane-wave distortions (or curvature of the incident ion trajectories near a target atom) does noticeably affect the cross sections, as in collisions of incident electrons with atoms, owing to the large mass and energy of the ion. In the method described here we have neglected the final-state interaction of the ejected electron with the ionizing ion. Methods are known for including this effect in the form of corrections to the

Born approximation, but its role is important only at relatively low energies $E \leqslant 1$ MeV/nucleon.

The accuracy of the calculation is mainly determined by the use of the Coulomb wave functions (2.7) and (2.8) and the sum rule (3.1)–(3.3) and (3.18)–(3.20). The Coulomb wave functions (2.7) and (2.8) made it possible to obtain analytic expressions for the ionization matrix elements and the form factors. These calculations must be repeated when other wave functions are used. Study of the sum rule in the simplest case, that of ionization of the H atom in collisions with H atoms, has shown that modification of the sum rule leads to a significant difference in the value of the total ionization cross section only at energies $E \leqslant 200$ keV/nucleon.

In conclusion, the authors would like to thank A. M. Baldin and E. D. Donets for useful remarks and discussions.

APPENDIX

The values of the matrix elements $L(nlm, n'l'm')$ are as follows:

$$L(1s, 1s)=\frac{1}{(1+\alpha_1^2)^2}, \quad \alpha_1=\frac{qz^*}{2z_{1s}}, \tag{A1}$$

$$L(2s, 2s)=\frac{1-3\alpha_2^2+2\alpha_2^4}{(1+\alpha_2^2)^4}, \quad \alpha_2=\frac{qz^*}{z_{2s}}, \tag{A2}$$

$$L(2p_0, 2p_0)=\frac{1-5\alpha_3^2}{(1+\alpha_3^2)^4}, \quad \alpha_3=\frac{qz^*}{z_{2p}}, \tag{A3}$$

$$L(2p_1, 2p_1)=\frac{1}{(1+\alpha_3^2)^3},$$

$$L(1s, 2s)=\frac{c}{\sqrt{1-c^2}}\left[\frac{1+\alpha_4^2(z_{1s}+z_{2s})(z_{1s}-z_{2s})^{-1}}{(1+\alpha_4^2)^3} - \frac{1}{(1+\alpha_1^2)^2}\right], \tag{A4}$$

$$C=\frac{\sqrt{8z_{1s}^3z_{2s}^3}(z_{1s}-z_{2s})}{(z_{1s}+\frac{1}{2}z_{2s})^4}, \quad \alpha_4=\frac{qz^*}{(z_{1s}+\frac{1}{2}z_{2s})}, \tag{A5}$$

$$L(1s, 2p_0)=\frac{\sqrt{2^5z_{1s}^3z_{2p}^5}\alpha_5}{(z_{1s}+\frac{1}{2}z_{2p})^4(1+\alpha_5^2)^3}, \quad \alpha_5=\frac{qz^*}{(z_{1s}+\frac{1}{2}z_{2p})},$$

$$L(2s, 2p_0)=\frac{2^5\alpha_6\sqrt{z_{2s}^3z_{2p}^5}[2z_{2s}(\alpha_6^2-2)+z_{2p}(1+\alpha_6^2)]}{(z_{2s}+z_{2p})^5(1+\alpha_6^2)^4}, \tag{A6}$$

$$\alpha_6=\frac{2qz^*}{(z_{2s}+z_{2p})}. \tag{A7}$$

[1] V. G. Andreev *et al.*, in *Proceedings of the Tenth Intern. Conf. on Charged-Particle Accelerators* [in Russian], Protvino, 1977, Vol. 1, p. 273.

[2] A. A. Vasil'ev, in *Proceedings of the Sixth All-Union Meeting on Charged-Particle Accelerators* [in Russian], Dubna, 1979, Vol. 1, p. 37.

[3] A. A. Vasil'ev and A. K. Kaminskiĭ, in *Lectures at the Fourth All-Union School on the Physics of Electron and Atom Collisions* [in Russian] (Moscow State University Press, Moscow, 1978), p. 246.

[4] *Catalogue of High Energy Accelerators, Fourteenth Intern. Conference on High-Energy Accelerators*, Tsukuba, Japan, 1989.

[5] T. L. Hardt and R. L. Watson, At. Data Nucl. Data Tables **17**, 107 (1976).

[6] R. C. Dehmel, H. K. Chau, and H. H. Fleischmann, At. Data **5**, 231 (1973).

[7] H. D. Betz, Rev. Mod. Phys. **44**, 465 (1972).

[8] C. H. Rutledge and R. L. Watson, At. Data Nucl. Data Tables **12**, 195 (1976).

[9] A. K. Kaminskiĭ, R. A. Meshcherov, and V. S. Nikolaev, Tr. Radiotekh. Inst. Akad. Nauk SSSR No. 16, 330 (1973) [in Russian].

[10] A. A. Vasil'ev, I. S. Dmitriev, A. K. Kaminskiĭ, and V. S. Nikolaev, Tr. Radiotekh. Inst. Akad. Nauk SSSR No. 22, 200 (1975) [in Russian].

[11] R. D. DuBois, L. H. Toburen, M. E. Middendorf, and O. Jagutzuki, Phys. Rev. A **49**, 350 (1994).

[12] V. P. Shevelko, AIP Conference Proceedings Vol. 295 (AIP, New York, 1993), p. 558.

[13] A. M. Baldin, Fiz. Élem. Chastits At. Yadra **8**, 429 (1977) [Sov. J. Part. Nucl. **8**, 175 (1977)].

[14] E. D. Donets, in *Proceedings of the Fifth All-Union Meeting on Charged-Particle Accelerators* [in Russian], Dubna, 1977, Vol. 1, p. 346.

[15] T. A. Antaya and S. Gamino, in *Proceedings of the Intern. Workshop on Strong Microwaves in a Plasma*, Nizhny Novgorod, 1994, p. 399.

[16] P. Sortais, in *Proceedings of the Intern. Workshop on Strong Microwaves in a Plasma*, Nizhny Novgorod, 1994, p. 312.

[17] A. K. Kaminskiĭ, R. A. Meshcherov, and M. I. Popova, Tr. Radiotekh. Inst. Akad. Nauk SSSR No. 22, 215 (1975) [in Russian].

[18] A. K. Kaminskiĭ, R. A. Meshcherov, V. S. Nikolaev, and M. I. Popova, Tr. Radiotekh. Inst. Akad. Nauk SSSR No. 16, 318 (1973) [in Russian].

[19] A. A. Vasil'ev, A. K. Kaminskiĭ, R. A. Meshcherov, V. S. Nikolaev, and M. I. Popova, in *Proceedings of the Fourth All-Union Meeting on Charged-Particle Accelerators* [in Russian], Moscow, 1975, Vol. 1, p. 262.

[20] Yu. V. Bulgakov, A. K. Kaminskiĭ, S. V. Lovstov, and R. A. Meshcherov, Tr. Radiotekh. Inst. Akad. Nauk SSSR No. 30, 61 (1977) [in Russian].

[21] A. K. Kaminsky, R. A. Meshcherov, and M. I. Popova, Nucl. Instrum. Methods **137**, 183 (1976).

[22] A. K. Kaminsky, R. A. Meshcherov, M. I. Popova, and V. D. Sazhin, Nucl. Instrum. Methods **180**, 231 (1981).

[23] A. K. Kaminsky and M. I. Popova, in *Proceedings of the Eighth All-Union Meeting on Charged-Particle Accelerators* [in Russian], Dubna, 1983, Vol. 1, p. 348.

[24] R. L. Martin and R. Arnold, Nucl. Instrum. Methods **155**, 337 (1978).

[25] R. L. Martin, R. Arnold, R. Burke, and J. Watson, in *Proceedings of the Seventh All-Union Meeting on Charged-Particle Accelerators* [in Russian], Dubna, 1981, Vol. 2, p. 362.

[26] S. Humphries, Jr., J. Plasma Phys. Thermonucl. Fusion **20**, 1549 (1980).

[27] G. Yonas, Sci. Am. **239**, No. 5, 40 (1978).

[28] C. Rubbia, Nuovo Cimento A **106**, 1429 (1993).

[29] V. G. Vasil'kov, V. I. Gol'danskiĭ, V. P. Dzhelepov, and V. P. Dmitrievskiĭ, At. Energ. **29**, No. 3, 151 (1970) [in Russian].

[30] A. A. Vasil'ev, R. G. Vasil'kov, B. L. Ioffe *et al.*, in *Proceedings of the Sixth All-Union Meeting on Charged-Particle Accelerators* [in Russian], Dubna, 1979, Vol. 1, p. 236.

[31] *Proceedings of Advanced Nuclear Energy Research, Evaluation by Accelerators*, Mito, Japan, 1990.

[32] V. S. Barashenkov, L. G. Levchuk, Zh. Zh. Musul'manbekov *et al.*, At. Energ. **61**, No. 1 (1986) [in Russian].

[33] P. P. Blagovolin, V. D. Dubinskiĭ, V. D. Kazaritskiĭ *et al.*, At. Energ. **66**, No. 5 (1988) [in Russian].

[34] L. D. Tolstov, Preprint 18-89-778, JINR, Dubna (1989) [in Russian].

[35] L. D. Tolstov, Preprint 18-92-303, JINR, Dubna (1992) [in Russian].

[36] K. D. Tolstov, JINR Rapid Commun. **5**, No. 62, 5 (1993).

[37] *Proceedings of the Workshop on Nuclear Transmission of Long-Lived Nuclear Power Radiowastes*, Obninsk, Russia, 1991.

[38] G. Van Tuyle, *Project PHONIX—Proposal of Long-Lived Radioactive Wastes to Produce Electric Power*, Brookhaven National Laboratory (1992).

[39] F. Carminati, C. Gels, R. Klapisch *et al.*, Preprint CERN/AT/93-47/(ET), CERN, Geneva (1993).

[40] C. Rubbia *et al.*, in *Proceedings of the Intern. Conf. on Accelerator-Driven Transmutation Technologies and Applications*, Las Vegas, 1994, AIP Conference Proceedings No. 346 (AIP, New York).

[41] *The Atomic Energy Industry Radioactive Waste Handling Problem*, ISB

N5-201-09424, Moscow Physico-Technical Institute, USSR Academy of Sciences, Moscow (1991).
[42] Yu. M. Ado, V. P. Kryuchkov, and V. N. Lebedev, At. Energy **77**, No. 4, 300 (1994) [in Russian].
[43] R. Fernandez, P. Mandrillon, C. Rubbia, and J. A. Rubbia, Report CERN/LHC/96-01 (EET), CERN, Geneva (1996).
[44] V. P. Dmitrievskiĭ, Fiz. Élem. Chastits At. Yadra **28**, 815 (1997) [Phys. Part. Nuclei **28**, 322 (1997)].
[45] I. V. Chuvilo, in *Proceedings of the Conf. AOTT-94*, Las Vegas, 1994, p. 248.
[46] G. I. Batskikh *et al.*, in *Proceedings of the Conference IPAC-95*, Dallas, 1995.
[47] N. Fietier and P. Mandrillon, Report CERN/AT/95-03 (ET) (Revised), CERN, Geneva (1995).
[48] I. A. Shelaev, Kratk. Soobshch. OIYaI (Dubna) 5(62)-93 (1993) [in Russian].
[49] U. Trinks, in *Proceedings of the Fourteenth Cyclotron Conference*, Cape Town, 1995.
[50] E. Esaray, Ph. Sprangle, J. Krall, and A. Ting, IEEE Trans. Plasma Sci. **24**, No. 2 (1996).
[51] A. K. Kaminskiĭ, in *Lectures Presented at the Fourth All-Union School on the Physics of Electron and Atom Collisions* [in Russian] (Moscow State University Press, Moscow, 1978), p. 171.
[52] N. M. Kabachnik, Nucl. Instrum. Methods B **115**, 298 (1996).
[53] G. N. Flerov, in *Proceedings of the Seventh All-Union Meeting on Charged-Particle Accelerators* [in Russian], Dubna, 1981, Vol. 2, p. 203.
[54] A. I. Ruderman, in *Proceedings of the Seventh All-Union Meeting on Charged-Particle Accelerators* [in Russian], Dubna, 1981, Vol. 2, p. 215.
[55] L. L. Gol'din, I. V. Chuvilo, and I. A. Ruderman, in *Proceedings of the Fourth Meeting on the Use of New Nuclear Physics Methods to Solve Technical and Economic Problems* [in Russian], Dubna, 1978, p. 329.
[56] I. V. Chuvilo, in *Proceedings of the Fifth All-Union Meeting on Charged-Particle Accelerators* [in Russian], Moscow, 1977, Vol. 2, p. 139.
[57] S. N. Dmitriev and N. G. Zaĭtseva, Fiz. Élem. Chastits At. Yadra **27**, 977 (1996) [Phys. Part. Nuclei **27**, 403 (1996)].
[58] W. K. Chu, J. Mayer, and M.-A. Nicolet, *Backscattering Spectrometry* (Academic Press, New York, 1978).
[59] L. C. Feldman, J. W. Mayer, and S. T. Picraux, *Materials Analysis by Ion Channeling* (Academic Press, New York, 1982).
[60] B. H. Bransden, *Atomic Collision Theory* (Benjamin, New York, 1970).
[61] W. E. Meyerhof and Taulbjerg, Annu. Rev. Nucl. Sci. **2**, 279 (1977).
[62] A. S. Davydov, *Quantum Mechanics*, 2nd ed. (Pergamon Press, Oxford, 1976) [Russ. original, GIFML, Moscow, 1963].
[63] A. K. Kaminskiĭ and M. I. Popova, Zh. Tekh. Fiz. **56**, 1287 (1986) [Sov. Phys. Tech. Phys. **31**, 754 (1986)].
[64] A. R. Edmonds, *Angular Momentum in Quantum Mechanics* (Princeton University Press, Princeton, 1957), p. 57.
[65] H. Levy, Phys. Rev. **185**, 7 (1969).
[66] Y. K. Kim and M. Inokuti, Phys. Rev. **165**, 39 (1968).
[67] D. T. J. Cromer, Chem. Phys. **50**, 4857 (1969).
[68] M. Naon, M. Carnille, and Y. K. Kim, J. Phys. B **8**, 684 (1975).
[69] *International Tables for X-Ray Crystallography* (Kynoch Press, Birmingham, England, 1968), No. 3.
[70] A. K. Kaminskiĭ, Brief Commun. N1(81)-97, JINR, Dubna (1997)) [in Russian].
[71] K. Omidvar, H. L. Kyle, and E. C. Sullivan, Phys. Rev. A **5**, 1174 (1972); (a) L. S. Bartel and R. M. Javin, J. Chem. Phys. **43**, 865 (1965).
[72] T. A. Carlson, C. W. Nestor, N. Wasserman *et al.*, At. Data **2**, 63 (1970).
[73] K. D. Sevier, At. Data Nucl. Data Tables **24**, 323 (1979).
[74] S. P. Ahlen, Rev. Mod. Phys. **52**, 121 (1980).
[75] M. H. J. Day, J. Phys. B **14**, 231, 56 (1981).
[76] L. D. Landau and E. M. Lifshitz, *Quantum Mechanics: Non-Relativistic Theory*, 3rd ed. (Pergamon Press, Oxford, 1977) [Russ. original, GIFML, Moscow, 1963].
[77] B. H. Choi, E. Merzbacher, and G. S. Khandelwal, At. Data **5**, 291 (1973).
[78] B. H. Choi, Phys. Rev. A **7**, 2056 (1973).
[79] M. Inokuti, Rev. Mod. Phys. **43**, 297 (1971).
[80] A. K. Kaminsky and M. I. Popova, in *Abstracts of Contributed Papers of the Fourteenth ICPEAC*, Palo Alto, 1985, p. 504.
[81] A. K. Kaminsky, N. G. Myakishev, and M. I. Popova, J. Phys. B **13**, 1161 (1980).
[82] A. K. Kaminsky and M. I. Popova, J. Phys. B **15**, 403 (1982).
[83] F. Drepper and J. S. Briggs, J. Phys. B **9**, 2063 (1982).
[84] L. H. Toburen, Phys. Rev. A **3**, 2166 (1971).
[85] W. E. Wilson and L. H. Toburen, Phys. Rev. A **7**, 1535 (1973).
[86] A. K. Kaminskiĭ, Kratk. Soobshch. OIYaI No. 4(84)-97, 21 (1997) [in Russian].
[87] B. H. Bransden, J. J. Smith, and K. H. Winters, J. Phys. B **11**, 3095 (1978).
[88] R. Biswas and C. Sinha, J. Phys. B **28**, 1311 (1995).
[89] R. Biswas and C. Sinha, Phys. Rev. A **51**, 3766 (1995).
[90] A. K. Kaminsky and M. I. Popova, J. Phys. B **9**, L177 (1976).
[91] R. E. Olson, J. Wang, and J. Ullrich, AIP Conference Proceedings No. 295 (AIP, New York, 1993), p. 520.
[92] Y. Fisher, Yu. Ralchenko, A. Goldrich *et al.*, J. Phys. B **28**, 3227 (1995).
[93] J. H. McGuire, N. Berrach, J. A. R. Samson *et al.*, J. Phys. B **28**, 913 (1995).
[94] L. P. Presnyakov, H. Tawara, I. Yu. Tolstikhina *et al.*, J. Phys. B **28**, 785 (1995).
[95] E. S. Solov'ev, R. N. Il'in, V. A. Oparin *et al.*, Zh. Éksp. Teor. Fiz. **42**, 659 (1962) [Sov. Phys. JETP **15**, 459 (1962)].
[96] J. Wexler, J. Chem. Phys. **41**, 1714 (1965).
[97] V. V. Afrosimov, Yu. A. Mamaev, M. H. Panov *et al.*, Zh. Tekh. Fiz. **39**, 159 (1969) [Sov. Phys. Tech. Phys. **14**, 104 (1969)].
[98] L. J. Puckett and D. W. Martin, J. Chem. Phys. A **1**, 1432 (1970).
[99] E. C. Montenegro and W. E. Meyerhof, Phys. Rev. A **43**, 2289 (1991).

Translated by Patricia A. Millard